Eta-1 (Osteopontin): An Early Component of Type-1 (Cell-Mediated) Immunity

Samy Ashkar,[1]* Georg F. Weber,[2,3]*† Vassiliki Panoutsakopoulou,[2,4] Marie E. Sanchirico,[2,4] Marianne Jansson,[2,4] Samer Zawaideh,[1] Susan R. Rittling,[5] David T. Denhardt,[5] Melvin J. Glimcher,[1] Harvey Cantor[2,4]‡

Cell-mediated (type-1) immunity is necessary for immune protection against most intracellular pathogens and, when excessive, can mediate organ-specific autoimmune destruction. Mice deficient in Eta-1 (also called osteopontin) gene expression have severely impaired type-1 immunity to viral infection [herpes simplex virus–type 1 (KOS strain)] and bacterial infection (*Listeria monocytogenes*) and do not develop sarcoid-type granulomas. Interleukin-12 (IL-12) and interferon-γ production is diminished, and IL-10 production is increased. A phosphorylation-dependent interaction between the amino-terminal portion of Eta-1 and its integrin receptor stimulated IL-12 expression, whereas a phosphorylation-independent interaction with CD44 inhibited IL-10 expression. These findings identify Eta-1 as a key cytokine that sets the stage for efficient type-1 immune responses through differential regulation of macrophage IL-12 and IL-10 cytokine expression.

The development of cell-mediated (type-1) immune responses is necessary for protection against the growth of many infectious pathogens and, when excessive, can mediate autoimmune host tissue destruction. Although macrophage activation by microbial pathogens (*1, 2*) and foreign body reactions (*3*) are associated with type-1 immunity, the cellular and molecular events that imprint this response are not fully understood. An essential early step in this process is macrophage production of IL-12 at sites of infection, whereas early IL-10 production inhibits this response (*4*). Although IL-12 responses can be triggered by an interaction between the CD40 ligand on activated T cells and CD40 on macrophages (*4*), this interaction also induces the inhibitory IL-10 cytokine (*5, 6*), and its transient nature may not suffice for sustained IL-12 induction in vitro (*7*) or in vivo (*8*).

A gene product that may play an important role in the development of type-1 immunity is the T cell cytokine Eta-1 (for early T lymphocyte activation–1), also known as osteopontin (Opn) (*9*). The Eta-1 gene is expressed in T cells early in the course of bacterial infections (within 48 hours), and interaction of its protein product with macrophages can induce inflammatory responses (*10*). Genetic resistance to infection by certain strains of *Rickettsia* may depend on Eta-1–dependent attraction of monocytes into infectious sites and acquisition of bacteriocidal activity (*11*); the granulomatous responses characteristic of sarcoidosis and tuberculosis are associated with high levels of Eta-1 expression (*12*).

Granuloma formation in these human diseases is a cellular consequence of type-1 immunity (*12*), and sarcoid-type granulomas can be induced in mice after injection of polyvinyl pyrrolidone (PVP) (*13*). Because certain murine models of parasite-induced granulomas may reflect a mixture of type-2 and type-1 immunity (*6*), we first established the importance of IL-12–dependent type-1 immunity in this murine model of granuloma formation. An intense granulomatous response was provoked shortly after (subcutaneous) injection of PVP into C57BL/6 (+/+) but not C57BL/6 *nu/nu* strains of mice. This response was diminished by 70 to 80% in C57BL/6 IL-$12^{-/-}$ mice and was enhanced two- to threefold in C57BL/6 IL-$10^{-/-}$ mice (Fig. 1, A and B). Because C57BL/6 *nu/nu* mice coinjected with PVP and purified Eta-1 displayed a granulomatous reaction, this gene product can partially substitute for activated T lymphocytes in this setting (Fig. 1, A and B).

We then asked whether mice deficient in Eta-1 secondary to targeted gene mutation (*14*) formed granulomas after PVP injection. Eta-$1^{-/-}$ mice did not develop a detectable granulomatous response after challenge with PVP; the response was partially restored by coinjection of purified Eta-1 with PVP (Fig. 1, A and B). Histologic analysis of granulomas formed in Eta-$1^{+/+}$ mice and in Eta-$1^{-/-}$ mice reconstituted with purified Eta-1 revealed a similar macrophage-dominant cellular infiltrate: About 85% of granulomatous cells in both cases were Mac-1^+, whereas 5 to 10% were $CD3^+$ T cells or $B220^+$ B cells. BP-55^+ neutrophils, which were only a minor component (1 to 2%) of granulomas in these mice, increased 5- to 10-fold in the granulomas of IL-$10^{-/-}$ mice (Fig. 1C). Eta-$1^{-/-}$ mice also displayed defective granulomatous responses to injection of collagen and latex, consistent with reports that human T cells resident in sterile granulomas have high expression of Eta-1 (*12*). Restimulation of lymph nodes draining subcutaneous sites of PVP injection in Eta-$1^{-/-}$ mice and control mice with PVP revealed impaired IL-12 and interferon-γ (IFN-γ) responses: The IL-12 response was reduced by ~95%, and the IFN-γ response of Eta-$1^{-/-}$ mice was reduced by 90% in comparison to Eta-$1^{+/+}$ controls (Fig. 1D).

We next defined the role of Eta-1 in the immune response to herpes simplex virus–type 1 (HSV-1) (KOS strain) infection. Eta-$1^{-/-}$ mice infected by HSV-1 [4×10^6 plaque-forming units (PFU) via the cornea] did not develop a significant tuberculin-type delayed-type hypersensitivity (DTH) response after footpad challenge with HSV-1 (10^5 PFU), in contrast to the strong DTH response of Eta-$1^{+/+}$ controls (Fig. 2A, left). Although the numbers of T cells and proportions of T cell subsets in the thymus and peripheral lymphoid tissues of Eta-$1^{-/-}$ mice were similar to Eta-$1^{+/+}$ littermates (*15*), defective antiviral DTH responses might reflect a subtle alteration in lymphocyte or macrophage development. We therefore tested the effects of acute in vivo depletion of Eta-1 with a neutralizing antibody. Administration of antibody to Eta-1 (LF-123) (*16*) immediately before and repeatedly after HSV-1 infection efficiently inhibited the DTH response upon rechallenge (Fig. 2A, right).

Corneal HSV-1 infection can also lead to a destructive type-1 autoimmune inflammatory reaction, herpes simplex keratitis (HSK), initiated by CD4 cells that recognize a viral peptide mimic (*17*). This inflammatory response depends on the production of IL-12 and is inhibited by IL-10 (*18*). Within 10 to 14 days after corneal HSV-1 infection, ~65% of control Eta-$1^{+/+}$ mice developed HSK, whereas HSV-1–infected Eta-$1^{-/-}$ mice did not readily develop this disease (Fig. 2B). Analysis of cells from the draining lymph nodes of virus-infected Eta-$1^{-/-}$ and Eta-$1^{+/+}$ mice indicated that they responded similarly to HSV-1 according to [^{3}H]thymidine incorporation after viral restimu-

[1]Laboratory for Skeletal Disorders and Rehabilitation, Department of Orthopedic Surgery, Children's Hospital, Harvard Medical School, 300 Longwood Avenue, Boston, MA 02115, USA. [2]Department of Cancer Immunology and AIDS, Dana-Farber Cancer Institute; [3]Department of Medicine; [4]Department of Pathology; Harvard Medical School, 44 Binney Street, Boston, MA 02115, USA. [5]Faculty of Arts and Sciences, Division of Life Sciences, Rutgers University, 604 Allison Road, NJ 08854, USA.

*These authors contributed equally to this work.
†Present address: Division of Radiation and Cancer Biology, New England Medical Center, 750 Washington Street, Boston, MA 02111, USA.
‡To whom correspondence should be addressed. E-mail: Harvey_Cantor@DFCI.harvard.edu

lation in vitro (*19*). However, draining lymph node cells from virally infected Eta-$1^{-/-}$ mice produced exaggerated amounts of IL-10 and IL-4 and reduced IL-12 in comparison with Eta-$1^{+/+}$ controls (Fig. 2C). In contrast with this sterile granulomatous response, IFN-γ levels were not reduced in Eta-$1^{-/-}$ mice after HSV-1 viral infection (*20*), consistent with an IL-12–independent pathway to IFN-γ production that may depend on virally induced IFN-α/β production (*21*).

We then investigated the ability of Eta-$1^{-/-}$ mice to mount a protective immune response after bacterial infection. The murine response to *Listeria monocytogenes* is an experimental cornerstone of our understanding of the early events leading to type-1 immunity after microbial infection (*1*) and depends on early macrophage production of IL-12 and downstream expression of IFN-γ (*22*). Eta-$1^{-/-}$ mice were defective in their ability to clear *L. monocytogenes* after systemic infection, similar to the defect in IL-$12^{-/-}$ mice (*23*) (see Web figure 1, available at www.sciencemag.org/feature/data/1046451.shl). Restimulation of spleen cells from Eta-$1^{-/-}$ and Eta-$1^{+/+}$ mice with heat-killed bacteria revealed that cells from the former mice had reduced IFN-γ responses: 25.5 ± 6.5 ng/ml of IFN-γ were produced by spleen cells from Eta-$1^{+/+}$ mice in comparison with 3.2 ± 1.2 ng/ml of IFN-γ from Eta-$1^{-/-}$ mice (*24*).

Thus, Eta-1 expression may affect type-1 immunity through regulation of the IL-12 and IL-10 cytokine ratio. To define the effect of Eta-1 on IL-10 and IL-12 production by macrophages in vitro, we incubated resident peritoneal macrophages with increasing concentrations of purified Eta-1 in serum-free medium (Fig. 3A). This resulted in the secretion of as much as 400 pg/ml of IL-12 at 48 hours, whereas IL-10 production was not detected (Fig. 3, A and B). The failure of Eta-1 to induce IL-10 was somewhat surprising because other cytokines that activate macrophages, including tumor necrosis factor–α, IL-1, IL-2, IL-3, and IL-6, all stimulate IL-10 secretion (*25*), and lipopolysaccharide (LPS) stimulation of these resident peritoneal macrophages induced both IL-12 (~250 pg/ml) and IL-10 (~100 pg/ml) (Fig. 3B). Further analysis showed that Eta-1 actively suppressed the LPS-dependent IL-10 response of resident peritoneal macrophages by 80 to 95% (Fig. 3C).

The interaction of Eta-1 with macrophages is mediated through two functional receptors. Engagement of CD44 mediates chemotactic migration (*26*), and interaction with $\alpha_V\beta_3$ integrin causes haptotaxis, adhesion, and spreading (*10, 27*). We asked which receptor was responsible for the regulation of macrophage cytokine production by Eta-1. Induction of IL-12 is inhibited by GRGDS (*28*) peptide (but not GRADS peptide) (*29*) and by antibody to the integrin β_3 subunit (but not by antibody to CD44), and macrophages from CD44$^{-/-}$ mice

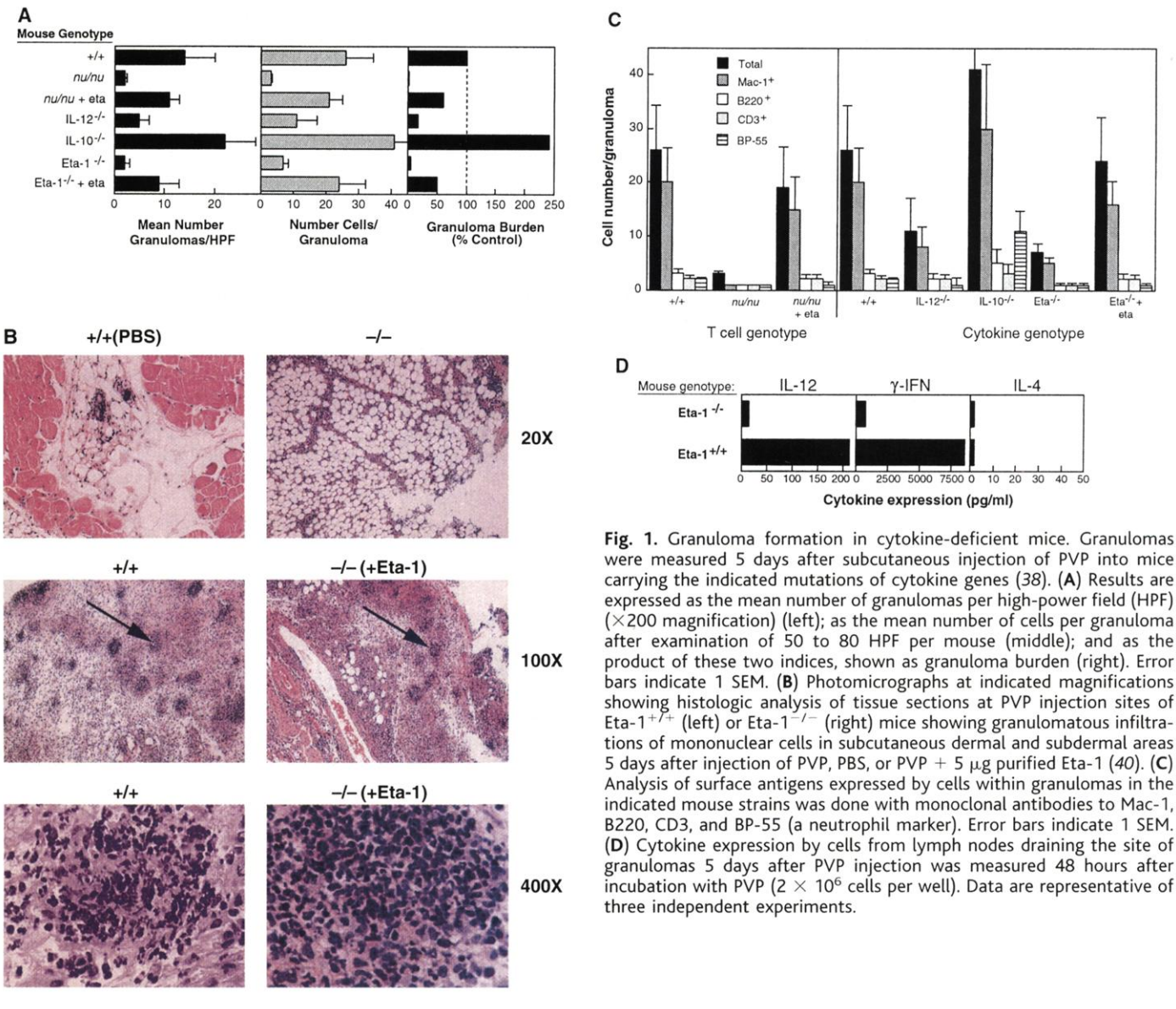

Fig. 1. Granuloma formation in cytokine-deficient mice. Granulomas were measured 5 days after subcutaneous injection of PVP into mice carrying the indicated mutations of cytokine genes (*38*). (**A**) Results are expressed as the mean number of granulomas per high-power field (HPF) (×200 magnification) (left); as the mean number of cells per granuloma after examination of 50 to 80 HPF per mouse (middle); and as the product of these two indices, shown as granuloma burden (right). Error bars indicate 1 SEM. (**B**) Photomicrographs at indicated magnifications showing histologic analysis of tissue sections at PVP injection sites of Eta-$1^{+/+}$ (left) or Eta-$1^{-/-}$ (right) mice showing granulomatous infiltrations of mononuclear cells in subcutaneous dermal and subdermal areas 5 days after injection of PVP, PBS, or PVP + 5 μg purified Eta-1 (*40*). (**C**) Analysis of surface antigens expressed by cells within granulomas in the indicated mouse strains was done with monoclonal antibodies to Mac-1, B220, CD3, and BP-55 (a neutrophil marker). Error bars indicate 1 SEM. (**D**) Cytokine expression by cells from lymph nodes draining the site of granulomas 5 days after PVP injection was measured 48 hours after incubation with PVP (2×10^6 cells per well). Data are representative of three independent experiments.

(*30*) display an unimpaired IL-12 response (Fig. 4, A to C). Moreover, Eta-1–dependent induction of IL-12 secretion from macrophages was not due to contamination with endotoxin: *Limulus* lysate analysis indicated that purified Eta-1 contained <1 ng/g of endotoxin, and the IL-12 response of macrophages from C3H.HeJ mice (which are defective in endotoxin receptor-mediated signaling) was not obviously impaired in comparison to other strains (Fig. 4C). In contrast to IL-12 induction, inhibition of IL-10 depends on engagement of the CD44 receptor: Eta-1–dependent inhibition of IL-10 is blocked by antibody to CD44 but not by antibody to integrin β_3, and macrophages from CD44$^{-/-}$ mice are resistant to Eta-1 inhibition of the IL-10 response (Fig. 4, A to C). To further characterize the RGD-dependent interaction with the macrophage integrin receptor, we analyzed fragments from an Eta-1 Lys-C digest and identified a proteolytic fragment from the NH_2-terminal portion of Eta-1, which contains the integrin binding site (termed NK10) that is sufficient to induce macrophage IL-12 expression (Fig. 4A).

Eta-1 is secreted in nonphosphorylated and phosphorylated forms (*31*). Phosphorylation may allow Eta-1 to associate with the cell surface rather than the extracellular matrix (*32*), through a contribution to integrin binding. In contrast, serine phosphorylation of recombinant Eta-1 is not required for CD44-dependent interactions leading to chemotactic migration (*26*). We investigated whether phosphorylation of Eta-1 might affect its ability to regulate IL-12 and IL-10 expression. Dephosphorylation of purified, naturally produced Eta-1 abolished IL-12 stimulatory activity; phosphorylation of recombinant Eta-1 at specific sites restored activity (*33*) (see Web figure 2, available at www.sciencemag.org/feature/data/1046451.shl). Although recombinant Eta-1–lacking phosphate groups could not induce IL-12, this molecule retained inhibitory activity for the macrophage IL-10 response (*33*). Thus, serine phosphorylation can provide molecular information that regulates the biological activity of a secreted protein.

Our data indicate that expression of Eta-1 represents an essential early step in the pathway that leads to type-1 immunity. Previous studies have established the importance of macrophage production of IL-12 in this pathway (*1, 4, 22*). Our experiments suggest that production of Eta-1 by activated T cells is an essential proximal event that potentiates the macrophage IL-12 response through integrin engagement and dampens the IL-10 response through CD44 engagement, leading to up-regulation of type-1 cytokines. The latter inhibitory effect on IL-10 may account for enhanced granulomatous responses of CD44$^{-/-}$ mice (*30*) and the finding that impairment of the granuloma response noted here is somewhat greater than might be anticipated from the response of IL-12–deficient mice (Fig. 1). These findings fill a logical gap in our understanding of the early molecular events that lead to type-1 immunity. Although down-regulation of CD40 ligand expression by IFN-γ and soluble CD40 occurs within 24 hours after viral infection, IL-12 is detected in serum over the next 7 to 10 days (*8*). Our experiments suggest that replacement of the CD40L signal by Eta-1 may potentiate the IL-12 response while dampening the IL-10 activity to allow full maturation of type-1 immunity, as judged by cellular responses and expression of downstream effector cytokines such as IFN-γ. The ability of an antigen to induce Eta-1 production after T cell receptor ligation may thus determine the ensuing duration and intensity of type-1 immune responses. Eta-1 imprinting of the IL-12 and IL-10 response after appropriate peptide stimulation (*34*) may also increase the likelihood of autoimmune sequelae as shown here (Fig. 2), through pathways that do not invariably require IFN-γ (*35*).

Eta-1–dependent regulation of two early cytokine checkpoints that dictate development of type-1 or type-2 immunity also suggests new therapeutic approaches to several diseases. Eta-1 analogs that mediate CD44-dependent inhibition of IL-10 may inhibit sepsis in burn patients (*36*), and Eta-1 antagonists may ameliorate the clinical course of bacterial arthritis (*37*). Engineered forms of

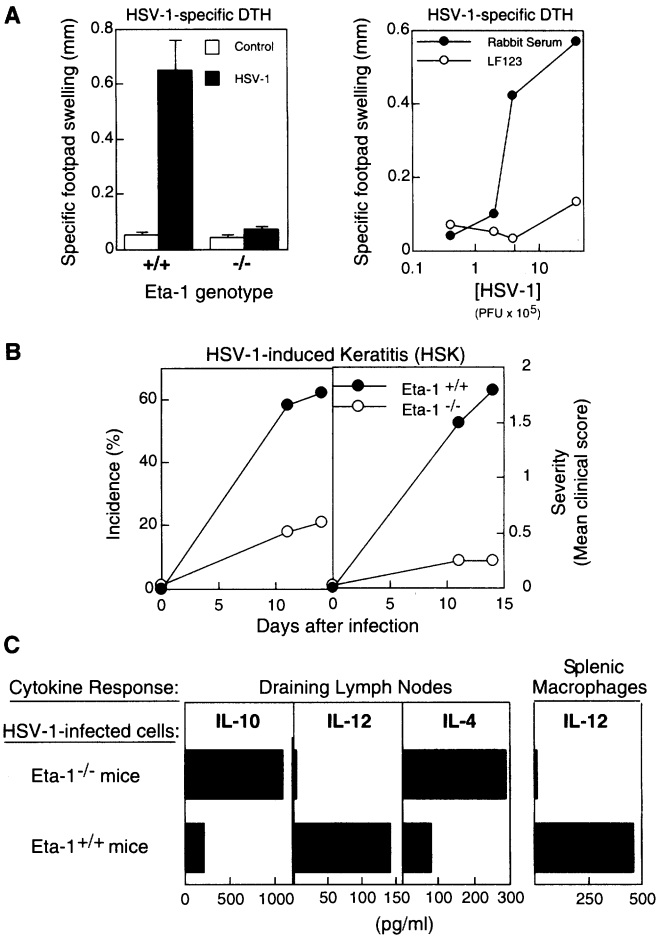

Fig. 2. The role of Eta-1 in immunity to HSV-1 (KOS strain). (**A**) (Left) Defective HSV-1–specific DTH responses in Eta-1$^{-/-}$ mice. C57BL/6 × 129 strain mice with or without a targeted disruption of the Eta-1 gene (–/–) or controls (+/+) were infected in the right eye with 4×10^6 PFU of HSV-1 (KOS) and challenged 5 days later in the left footpad with 1×10^5 PFU of UV-inactivated HSV-1 (KOS). The right (control) and left (HSV-1) footpads of each mouse were measured 24 hours later with a micrometer. Each data point represents the mean and standard error (error bars) of three mice per group. (Right) Inhibition of the anti–HSV-1 DTH response by acute depletion of Eta-1. The neutralizing antisera LF-123 (*16*) or control normal rabbit serum were injected at 25 μg per dose per day, starting 2 days before injection. On day 0, mice were infected with HSV-1 (KOS) and rechallenged 5 days later. The right and left footpads of each mouse were measured 24 hours after rechallenge, and specific swelling (left versus right footpad) is shown. (**B**) Development of HSK in Eta-1$^{-/-}$ mice. The right eyes of Eta-1$^{-/-}$ and Eta-1$^{+/+}$ mice were infected with 4×10^6 PFU of HSV-1 (KOS), and disease was assessed on days 11 and 14 after infection, as described (*17*). The severity of clinical stromal keratitis was scored on the basis of the percentage of corneal opacity: ≤25%, 1; ≤50%, 2; ≤75%, 3; and 75 to 100%, 4. Each point represents at least 16 mice and is the mean of three independent experiments. (**C**) Differential cytokine profile of draining lymph node cells and splenic macrophages from Eta-1$^{+/+}$ or Eta-1$^{-/-}$ mice after infection with HSV-1. Cytokine levels after restimulation of draining lymph node cells (from mice 15 days after HSV-1 infection in vivo) by 4×10^7 PFU of UV-inactivated HSV-1 using 48-hour supernatants were determined by ELISA (*19*). Viral restimulation of mixtures of purified lymph node T cells from virus-infected donors and syngeneic (nonimmune) adherent cells yielded less than one-third of the IL-10 response of mixtures of immune T cells and macrophages from draining lymph nodes of infected donors (*20*). The proliferative response of lymph node cells from HSV-1–infected Eta-1$^{+/+}$ and Eta-1$^{-/-}$ mice measured by [^{3}H]thymidine incorporation at 72 hours was 20.9×10^3 and 18.7×10^3 cpm, respectively.

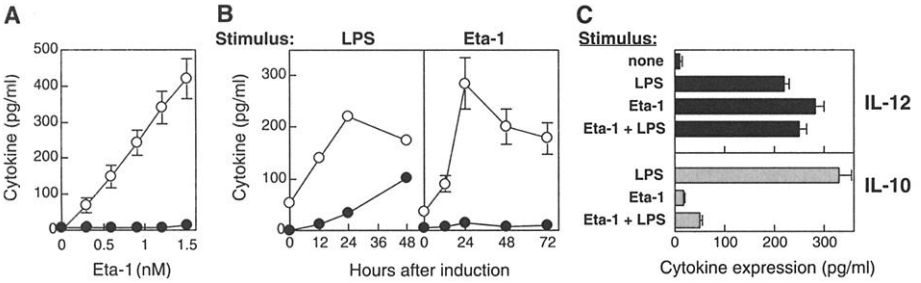

Fig. 3. Differential regulation of macrophage IL-12 and IL-10 responses by purified Eta-1. (**A**) Dose-dependent induction of IL-12 (open circles), but not IL-10 (solid circles) production, from macrophages by Eta-1. Resident peritoneal macrophages obtained from C57BL/6 mice (*41*) were incubated for 48 hours (5×10^5 macrophages per milliliter) with purified Eta-1 (*40*), and IL-10 and IL-12 p70 concentrations in the supernatant were determined by ELISA. Assays were done in quadruplets, and each point represents the mean and standard error (error bars) of three independent experiments. (**B**) Time course of IL-12 (open circles) p70 and IL-10 (solid circles) expression by resident peritoneal macrophages (5×10^5 macrophages per milliliter) after incubation with 5 nM Eta-1 or LPS (30 ng/ml). Assays were performed in quadruplets, and each data point represents the mean and standard error (error bars) of two independent experiments. (**C**) Inhibitory effect of Eta-1 on macrophage IL-10 production. Macrophages were activated with LPS (30 ng/ml) for 1 hour before addition of Eta-1 (5 nM) for an additional 48 hours and consecutive measurement of IL-12 and IL-10 by ELISA. Assays were performed in quadruplets, and each point represents the mean and standard error (error bars) of two independent experiments.

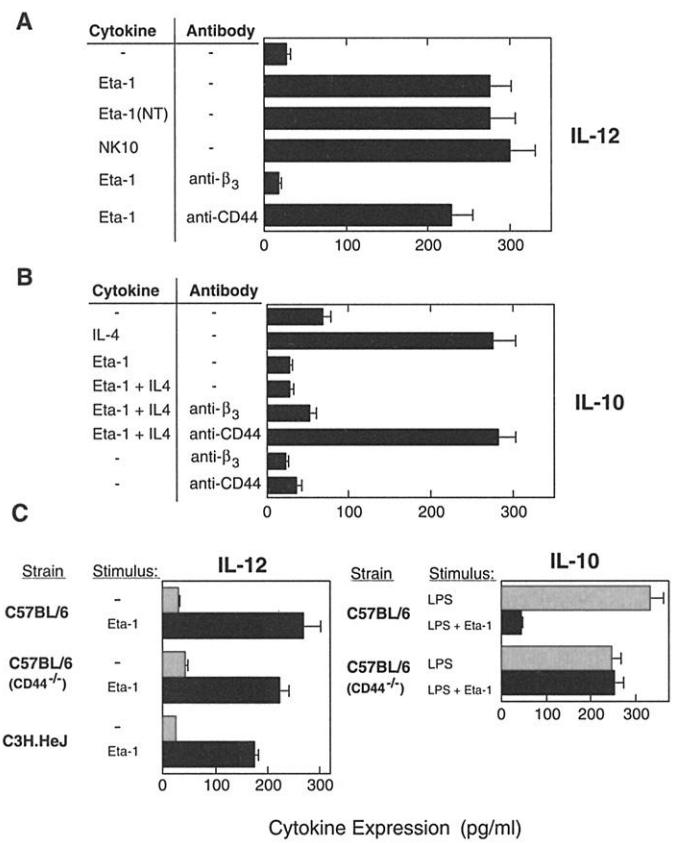

Fig. 4. Regulation of macrophage IL-12 and IL-10 expression by distinct Eta-1 receptors. (**A**) Secretion of IL-12 by macrophages is mediated by a 10-kD peptide (NK10) derived from the NH_2-terminal fragment of Eta-1 (*42*) and is inhibited by a blocking antibody to integrin β_3 (1 μg/ml), but is unaffected by antibody to CD44 (1 μg/ml). Error bars indicate 1 SEM. (**B**) Induction of IL-10 production by IL-4 (500 U/ml) in the presence or absence of purified Eta-1 (5 nM) and the effects of antibodies to CD44 [Km81 purified from TIB241 (*26*)] and the β_3 integrin (2C9.G2, PharMingen) are shown. Error bars indicate 1 SEM. (**C**) Production of IL-12 and IL-10 in response to Eta-1 by peritoneal macrophages from C57BL/6 mice, C57BL/6 mice that are deficient in CD44 gene expression (C57BL/6–CD44$^{-/-}$), and cells from C3H.HeJ mice. Mean values and standard errors (error bars) from at least four data points are shown.

Eta-1 that imprint type-1 responses after immunization may also be valuable components of viral and cancer vaccines.

References and Notes

1. E. R. Unanue, *Immunol. Rev.* **158**, 11 (1997).
2. R. Medzhitov and C. Janeway, *Semin. Immunol.* **10**, 351 (1998).
3. P. Matzinger, *Semin. Immunol.* **10**, 399 (1998).
4. C. M. Scheicher, M. Mehlig, H. P. Dienes, K. Reske, *Eur. J. Immunol.* **25**, 1566 (1995); S. E. Macatonia *et al.*, *J. Immunol.* **154**, 5071 (1995); K. M. Murphy, *Curr. Opin. Immunol.* **10**, 226 (1998).
5. F. Koch *et al.*, *J. Exp. Med.* **184**, 741 (1996).
6. A. O'Garra, *Immunity* **8**, 275 (1998).
7. F. Ria, G. Penna, L. Adorini, *Eur. J. Immunol.* **28**, 2003 (1998).
8. M. D. Sharma, M. L. de Moraes, F. Zavala, C. Pontoux, M. Papiernik, *J. Immunol.* **161**, 5357 (1998).
9. R. Patarca *et al.*, *J. Exp. Med.* **170**, 145 (1989); G. F. Weber, S. Ashkar, H. Cantor, *Proc. Assoc. Am. Physicians* **109**, 1 (1997); S. R. Rittling and D. T. Denhardt, *Exp. Nephrol.* **7**, 103 (1999).
10. R. P. Singh, R. Patarca, J. Schwartz, P. Singh, H. Cantor, *J. Exp. Med.* **171**, 1931 (1990); X. Q. Yu *et al.*, *Proc. Assoc. Am. Physicians* **110**, 50 (1998); D. T. Denhardt and M. Noda, *J. Cell. Biochem. Suppl.* **30/31**, 92 (1998).
11. R. Patarca, R. A. Saavedra, H. Cantor, *Crit. Rev. Immunol.* **13**, 225 (1993); T. J. Jerrells and J. V. Osterman, *Infect. Immun.* **31**, 1014 (1981).
12. G. J. Nau *et al.*, *Proc. Natl. Acad. Sci. U.S.A.* **94**, 6414 (1997); A. W. O'Regan *et al.*, *J. Immunol.* **162**, 1024 (1999).
13. C. van den Bogert *et al.*, *Virchows Arch.* **51**, 39 (1986).
14. C57BL/6 × 129/SV Eta-1$^{-/-}$ mice generated as described by S. R. Rittling *et al.* [*J. Bone Miner. Res.* **13**, 1101 (1998)] were compared to either Eta-1$^{+/+}$ littermates or age-matched C57BL/6 × 129/SV mice as controls.
15. T and B cell subsets in Eta-1$^{-/-}$ and Eta-1$^{+/+}$ littermates were as follows: C57BL/6 × 129 Eta-1$^{+/+}$ spleen, 93.7×10^6 total cells (30.8% CD3, 19.8% CD4, 11% CD8, and 49.7% B220); C57BL/6 × 129 Eta-1$^{-/-}$ spleen, 82.6×10^6 cells (27.8% CD3, 18.8% CD4, 9.0% CD8, and 55.5% B220); C57BL/6 × 129 Eta-1$^{+/+}$ lymph node, 32.0×10^6 cells (82.4% CD3, 42.8% CD4, 34.2% CD8, and 12.8% B220); and C57BL/6 × 129 Eta-1$^{-/-}$ lymph node, 21.9×10^6 cells (82.8% CD3, 49.3% CD4, 28.4% CD8, and 11.2% B220). T cells from Eta-1$^{-/-}$ and Eta-1$^{+/+}$ mice expressed levels of CD44 and CD62 that were not distinguishable. T cell expansion followed by apoptosis after superantigen (50 μg of staphylococcal enterotoxin B) intraperitoneal injection into Eta-1$^{-/-}$ and Eta-1$^{+/+}$ mice was indistinguishable at 3 days: +/+ $V_\beta 8^+$ CD4 cells (percentage of total spleen) increased from 3.6 to 5%; −/− $V_\beta 8^+$ CD4 cells increased from 3.2 to 5.5%; +/+ $V_\beta 6^+$ CD4 cells increased from 2.3 to 2.6%; −/− $V_\beta 6^+$ CD4 cells increased from 2.5 to 2.6%. Expression of IL-2 by lymph node and spleen T lymphocytes from Eta-1$^{-/-}$ and Eta-1$^{+/+}$ littermates in response to immobilized antibody to CD3 was also indistinguishable between the C57BL/6 × 129/SV Eta-1$^{-/-}$ and C57BL/6 × 129/SV Eta-1$^{+/+}$ mice.
16. L. W. Fisher, J. T. Stubbs, M. F. Young, *Acta Orthop. Scand.* **66**, 61 (1995).
17. Z.-S. Zhao, F. Granucci, L. Yeh, P. A. Schaffer, H. Cantor, *Science* **279**, 1344 (1998); A. C. Avery *et al.*, *Nature* **376**, 431 (1995).
18. J. W. Streilein, M. R. Dana, B. R. Ksander, *Immunol. Today* **18**, 443 (1997); M. Daheshia, N. Kuklin, S. Kanangat, E. Manickan, B. T. Rouse, *J. Immunol.* **159**, 1945 (1997).
19. HSV-1 stimulation of lymph node cells and splenic macrophages: The right superficial cervical draining lymph nodes of Eta-1$^{-/-}$ mice and Eta-1$^{+/+}$ littermate controls were harvested 15 days after infection of the right eye with 4×10^6 PFU of HSV-1 (KOS). Cells from these lymph nodes (2×10^6 cells per well) were incubated in the presence of 4×10^7 PFU of ultraviolet (UV)–inactivated HSV-1 (KOS). Supernatants harvested 48 hours later were tested for IL-10 and IL-12 p40 cytokine by sandwich enzyme-linked immunosorbent assay (ELISA) using OptEIA antibody sets (PharMingen, La Jolla, CA). IL-4 was measured after stimulation of draining lymph node cells by plate-bound antibody to CD3.
20. S. Ashkar *et al.*, data not shown.
21. A. Oxenius, U. Karrer, R. M. Zinkernagel, H. Hengartner, *J. Immunol.* **162**, 965 (1999); L. P. Cousens *et al.*, *J. Exp. Med.* **189**, 1315 (1999).
22. C. S. Tripp, S. F. Wolf, E. R. Unanue, *Proc. Natl. Acad. Sci. U.S.A.* **90**, 3725 (1993); C. S. Tripp, M. K. Gately, J. Hakimi, P. Ling, E. R. Unanue, *J. Immunol.* **152**, 1883 (1994); C. S. Tripp, O. Kanagawa, E. R. Unanue, *J. Immunol.* **155**, 3427 (1995).
23. *Listeria* infection and cytokine production were as followed. Virulent *L. monocytogenes* [strain 1778, American Type Culture Collection (ATCC) designation 43251] was grown in trypticase soy broth (Becton-Dickinson), and 10^3 colony-forming units (CFU),

a sublethal dose for this strain of *L. monocytogenes*, were injected intravenously. The titer of viable bacteria in the inoculum and in organ homogenates was determined by plating 10-fold serial dilutions on trypticase soy agar plates. Eta-$1^{-/-}$ mice contained liver-associated *Listeria*-infected cysts that were apparent 4 to 5 days after infection. Plates were incubated at 37°C, and the numbers of CFU were counted after 24 hours.

24. Spleen cells (4×10^6/ml) from four to five C57BL/6 × 129 Eta-$1^{+/+}$ or four to five C57BL/6 × 129 Eta-$1^{-/-}$ mice that had been intravenously inoculated 5 days earlier with 10^3 CFU were stimulated with heat-killed *L. monocytogenes* (2×10^8 CFU/ml) 96 hours before IFN-γ measurement by an OptEIA ELISA kit (PharMingen).
25. P. Stordeur *et al.*, *Mol. Immunol.* **32**, 233 (1995); P. Stordeur and M. Goldman, *Int. Rev. Immunol.* **16**, 501 (1998).
26. G. F. Weber, S. Ashkar, M. J. Glimcher, H. Cantor, *Science* **271**, 509 (1996).
27. L. Liaw *et al.*, *J. Clin. Invest.* **95**, 713 (1995); D. R. Senger *et al.*, *Am. J. Pathol.* **149**, 293 (1996).
28. Addition of 5 mM GRGDS peptide but not GRADS peptide (*29*) to cultures of peritoneal macrophages (*38*) resulted in an 80% reduction of the IL-12 response after LPS stimulation.
29. Single-letter abbreviations for the amino acid residues are as follows: A, Ala; D, Asp; E, Glu; G, Gly; L, Leu; N, Asn; P, Pro; Q, Gln; R, Arg; S, Ser; and T, Thr.
30. R. Schmits *et al.*, *Blood* **90**, 2217 (1997).
31. T. Kubota *et al.*, *Biochem. Biophys. Res. Commun.* **162**, 1453 (1989); A. F. Chambers, E. I. Behrend, S. M. Wilson, D. T. Denhardt, *Anticancer Res.* **12**, 43 (1992); E. S. Sorensen and T. E. Petersen, *Biochem. Biophys. Res. Commun.* **198**, 200 (1994); H. Salih, S. Ashkar, L. C. Gerstenfeld, M. J. Glimcher, *J. Biol. Chem.* **272**, 13966 (1997).
32. M. Nemir, M. W. DeVouge, B. B. Mukherjee, *J. Biol. Chem.* **264**, 18202 (1989); B. Ek-Rylander, M. Flores, M. Wendel, D. Heinegard, G. Andersson, *J. Biol. Chem.* **269**, 14853 (1994).
33. Dephosphorylation of Eta-1 is as follows. Five milligrams of purified Eta-1 was dephosphorylated using 6 U (60 U/mg) of type-II potato acid phosphatase (Sigma) as described (*39*). Phosphorylation of recombinant Eta-1:glutathione *S*-transferase (GST)–Eta-1 (5 mg) was phosphorylated as described [S. Ashkar, J. L. Schaffer, E. Salih, L. C. Gerstenfeld, M. J. Glimcher, *Ann. N.Y. Acad. Sci.* **760**, 296 (1995); (*27*)]. Phospho–amino acid analysis of the recovered protein revealed a phosphoserine content of 16 mol of phosphate per 1 mol of protein and 0.8 mol of phosphothreonine per 1 mol of protein.
34. S. L. Constant and K. Bottomly, *Annu. Rev. Immunol.* **15**, 297 (1999).
35. B. M. Segal, B. K. Dwyer, E. M. Shevach, *J. Exp. Med.* **187**, 537 (1998).
36. A. Lyons, J. L. Kelly, M. L. Rodrick, J. A. Mannick, J. A. Lederer, *Ann. Surg.* **226**, 450 (1997); J. L. Kelly, A. Lyons, C. C. Soberg, J. A. Mannick, J. A. Lederer, *Surgery* **122**, 146 (1997).
37. Z. Yin *et al.*, *Arthritis Rheum.* **40**, 1788 (1997).
38. PVP-dependent granulomas were formed as follows. C57BL/6 (+/+), C57BL/6 *nu/nu*, C57BL/6–IL-$12^{-/-}$ C57BL/6 × 129 Eta-$1^{+/+}$, and C57BL/6 ×129 Eta-$1^{-/-}$ mice were injected subcutaneously above the right hind limb with 500 μl of 0.5% PVP; C57BL/6 *nu/nu* and Eta-$1^{-/-}$ mice were coinjected with this inoculum of PVP and 10 μg of Eta-1 and purified as described below. After 5 days, mice were killed, tissue was extracted for histologic analysis, and local lymph nodes were obtained for cytokine expression. Samples were fixed in 10% buffered formalin and embedded in paraffin; 4- to 5-μm serial sections were stained with hematoxylin and eosin, and images were captured with a Sony DXC-970MD video camera and Optima 5.2 Histomorphometric analysis software.
39. S. Ashkar *et al.*, *Biochem. Biophys. Res. Comm.* **191**, 126 (1993).
40. Recombinant GST–Eta-1 fusion protein derived from *Escherichia coli* was digested with factor Xa and purified by affinity chromatography [S. Ashkar, M. J. Glimcher, R. A. Saavedra, *Biochem. Biophys. Res. Commun.* **194**, 274 (1993); (*39*)]. Briefly, native Eta-1 was isolated from MC3T3E1 cells or Ar5v T cells after concentration in PBS using a Millipore tangential flow system, applied to a Millipore LC100 equipped with a DEAE-Memsep 1000 cartridge, and developed in a discontinuous gradient of 0 to 1 M NaCl in phosphate buffer (pH 7.4). Eta-1–containing fractions were pooled (the major Eta-1 peak eluted at 0.26 M salt), concentrated by ultrafiltration, chromatofocused on mono P columns (Pharmacia) at pH 8.2, developed with polybuffer 74 (Pharmacia), and eluted from monobeads at pH 4.6. The eluted protein was judged to be pure by several criteria, including SDS electrophoresis and amino acid sequence analysis (NH_2-terminal and internal peptide analysis). Mass spectroscopic analysis revealed a peak centered around a mass of 35,400 daltons that was highly phosphorylated (11 mol of phosphate per 1 mol of protein), O-glycosylated but not N-glycosylated, and without measurable sulfate.
41. Resident peritoneal macrophages obtained by peritoneal lavage with phosphate-buffered saline (PBS) were treated with red cell lysis buffer and incubated (10^5 macrophages per 100 μl) for 2 hours. The adherent fraction was incubated with 5 nM Eta-1, LPS (30 ng/ml), or recombinant IL-4 (500 U/ml), or as indicated. Supernatant IL-10 or IL-12 p70 was assayed with commercial ELISA kits (R&D Systems, Minneapolis, MN), tested for viability by propidium iodide (>98%), and stained with fluorescein-conjugated antibody to Mac-1 (>98%). Blocking antibody to integrin β_3 was from PharMingen [J. F. Schultz and D. R. Armant, *J. Biol. Chem.* **270**, 11522 (1995)], and antibody to CD44, KM81 (ATCC), was used to block the interaction between CD44 and Eta-1 (*16*).
42. Although partial tryptic, chemotryptic, or Asp-N endopeptidase digestion of Eta-1 did not reveal an active peptide, a 10-kD fragment isolated from a Lys-C digest [NH_2-terminal sequence QETLPSN (*29*)] was active and predicted to terminate at the thrombin cleavage site. This 10-kD fragment contained ~5 mol of phosphate per 1 mol of peptide at seven potential phosphorylation sites.
43. Supported in part by NIH research grants AI12184, AI37833 (to H.C.), CA76176 (to G.F.W.), and AR34078 (to M.J.G.); grants AR44434, DC01295, ES06897 (to D.T.D.), and CA72740 (to S.R.R.) for development of Opn-null mice at Rutgers University; U.S. Department of Defense breast cancer grants DAMD17-98-1-8060 (to G.F.W.) and DAMD 17-99-1-9124 (to S.A.); U.S. Department of Public Health grant 340B9930002 and Biomorphics (to S.A.); the Fulbright Foundation (to S.Z.); and the Swedish Foundation for International Cooperation in Research and Higher Education (to M.J.). All experimentation involving animals was in accordance with Dana-Farber institutional guidelines. We thank T. W. Mak for CD$44^{-/-}$ mice; B. J. Rollins for *L. monocytogenes* strain 1778; S. Hikita and D. Block for technical assistance; and A. Angel, K. MacKay, and L. Lagasse for assistance in the preparation of the manuscript.

21 October 1999; accepted 15 December 1999

Synaptic Assembly of the Brain in the Absence of Neurotransmitter Secretion

Matthijs Verhage,[1,2,*] Ascanio S. Maia,[1] Jaap J. Plomp,[3] Arjen B. Brussaard,[4] Joost H. Heeroma,[1] Hendrika Vermeer,[1] Ruud F. Toonen,[1] Robert E. Hammer,[5] Timo K. van den Berg,[6] Markus Missler,[2†] Hans J. Geuze,[7] Thomas C. Südhof[2*]

Brain function requires precisely orchestrated connectivity between neurons. Establishment of these connections is believed to require signals secreted from outgrowing axons, followed by synapse formation between selected neurons. Deletion of a single protein, Munc18-1, in mice leads to a complete loss of neurotransmitter secretion from synaptic vesicles throughout development. However, this does not prevent normal brain assembly, including formation of layered structures, fiber pathways, and morphologically defined synapses. After assembly is completed, neurons undergo apoptosis, leading to widespread neurodegeneration. Thus, synaptic connectivity does not depend on neurotransmitter secretion, but its maintenance does. Neurotransmitter secretion probably functions to validate already established synaptic connections.

Synapses are focal points of communication between nerve cells. Together, billions of synapses account for the unique connectivity of the brain (*1*). To establish the synaptic network, outgrowing axons are precisely directed to their targets using a variety of guidance cues and recognition signals on the outgrowing axon and the target cell (*2*). Fusion of neurotransmitter vesicles at the axon tip is believed to supply the membrane for axonal outgrowth (*3*). The concomitant neurotransmitter release is thought to have a trophic role and to provide essential signals for the correct targeting of axons and synapse formation: Components of the presynaptic secretion machinery are already expressed in immature neurons before they differentiate (*4*). These components are targeted to the axon tip, where they are thought to be essential for axonal outgrowth in vitro (*3*, *5*). Outgrowing neurons have an active synaptic vesicle cycle, secrete neurotransmitters before synapse formation, and up-regulate this secretion once the growth cone comes close to its target (*6*). After synapses have formed, the secretion capacity of nerve terminals is up-regulated, and the Ca^{2+} affinity and tetanus toxin sensitivity increase.